DOI 10.1007/s10778-023-01176-3
International Applied Mechanics, Vol. 58, No. 5, September, 2022

COMPARISON OF THE EVOLUTION OF A SOLITARY ELASTIC CYLINDRICAL WAVE WITH FRIEDLANDER AND MACDONALD PROFILES*

J. J. Rushchitsky and V. M. Yurchuk

A nonlinear elastic cylindrical radial displacement wave is analyzed theoretically and numerically for an arbitrary solitary wave profile and initial wave profiles in the form of Friedlander and Macdonald functions. The five-constant Murnaghan model is used. Unlike the most profiles of nonlinear waves in materials that have periodical or single humps, these waves have no hump, decrease monotonically, and have concave downward profile. Both profiles are very similar, have the properties of solitary wave, and, therefore, can be studied using the nonlinear theory of elasticity. A comparison of the Macdonald and Friedlander profiles as the solutions of the linear wave equation for a cylindrical wave shows that if the Macdonald function is considered as the exact solution of this equation, then the Friedlander function can be considered an approximate solution of this equation because its graphical representation is similar to that of the Macdonald function. The evolution of waves is studied by the approximate method of limitation of displacement gradient taking into account the first two approximations. Formulas are theoretically obtained for an approximate representation of a solitary cylindrical wave and a concrete representation of this wave for the given Macdonald and Friedlander initial profiles. It is shown that the flection of the profiles changes when the waves propagate some distance but the behavior of the profiles (evolution scenarios) does not differ significantly from each other. Then within the framework of the problem stated, both profiles are interchangeable despite the fact that they are mathematically represented in different ways.

Keywords: solitary elastic cylindrical wave; Murnaghan five-constant potential; evolution; approximate method; Friedlander and Macdonald initial wave profiles

Introduction. We will study a displacement wave $u(x-vt)$ that is the solution of the nonlinear wave equation and has a profile such that it can be considered solitary.

Singular waves are known to be defined by their profile: it is described by either a finite function (nonzero on a finite interval) or a function of finite weight (the area under its graph remains constant on a finite interval outside which it can be neglected, i.e., the area (weight) is concentrated within a finite interval). A typical example of a solitary wave is a wave with Gauss profile (bell-shaped or hump-shaped wave described by a function of finite weight). The simplest solitary wave can be described by the classical d'Alembert solution $u(x,t)=f(x-vt)$ of the linear wave equation $u_{,tt}-v^2u_{,xx}=0$ for a one-dimensional displacement wave [2, 6, 9, 17].

S. P. Timoshenko Institute of Mechanics, National Academy of Sciences of Ukraine, 3 Nesterova St., Kyiv, Ukraine, 03057, e-mail: rushch@inmech.kiev.ua. Translated from Prykladna Mekhanika, Vol. 58, No. 5, pp. 16–26, September–October 2022. Original article submitted December 28, 2021.

* This study was sponsored by the budgetary program Support of Priority Areas of Research (KPKVK 6541230).

It should be noted that simple waves became classical in the second half of the 19th century and are still studied [7, 8, 13, 15].

The evolution (change in the initial profile during propagation) of a wave can be analyzed as a process occurring in either space or time. This follows from the fact that a wave is characterized by phase $\sigma = x - vt$, and if the wave velocity v is known, then a point in space corresponds to a fixed time point.

We will analyze the evolution of a cylindrical elastic wave using the Murnaghan five-constant model [1–3, 6, 16, 21]. The simplest nonlinear wave equation in the model includes quadratic nonlinearity only. It is quite difficult to analyze this equation for plane waves [2, 6, 9, 19, 20].

Since wave to be considered are cylindrical, we will use a quadratic nonlinear wave equations in cylindrical coordinates. Such an equation was used in [24, 25, 29, 30].

Let the cylindrical wave have a asymmetric initial profile described by the Friedlander and Macdonald functions. Unlike the majority of nonlinear waves in materials that have periodic or single humps, Friedlander and Macdonald waves do not have hump, decreases monotonically, and are convex down.

It should be noted that the Macdonald profile is natural for a cylindrical elastic wave and was studied earlier in [4, 5, 15, 30], whereas the Friedlander profile is typical for blast waves and was used to analyze a plane elastic wave [30]. The Friedlander profile is considered one of the simplest and often used to interpret experiments [10, 11, 14].

A common feature of both profiles is very similar graphic representations. However, the mathematical representations of these profiles are very different: the Friedlander profile is described by an ordinary function [9–11, 30]:

$$F\left[a(r - v_L t)\right] = A^o e^{-ba(r - v_L t)/x_{att}} \left[1 - a(r - v_L t)/x_{att}\right],$$

$$v_L = \sqrt{(\lambda + 2\mu)/\rho}, \tag{1}$$

and the Macdonald profile is described by a special function (Macdonald function):

$$K_0\left[a(r - v_L t)\right]. \tag{2}$$

Therefore, the question arises of how the difference between the mathematical representations influences the description of the wave evolution. This paper answers this question: the evolution scenarios are similar, yet different.

1. Statement of the Problem of the Propagation of a Cylindrical Radial Displacement Wave. A cylindrical radial elastic displacement wave is a wave that propagates in an unbounded elastic medium with a cylindrical circular cavity with a pulse applied to its boundary. The pulse excites axisymmetric motion in the radial direction. In the simplest case, the pulse is harmonic in time. The cylindrical coordinate system $Or\vartheta z$ is chosen so that the Oz-axis coincides with the axis of the cavity. Then the motion of the wave only depends on the radius r and time t. In terms of elasticity theory, the radial shear u_r and the three stress components $\sigma_{rr}, \sigma_{\vartheta\vartheta}, \sigma_{zz}$ are nonzero. The linear equation of motion has the following form [6, 17, 19]:

$$(\lambda + 2\mu)\left(u_{r,rr} + \frac{1}{r} u_{r,r} - \frac{u_r}{r^2}\right) = \rho u_{r,tt}. \tag{3}$$

The associated nonlinear equation in the Murnaghan model is the following [21, 30]:

$$(c_L)^{-2} u_{r,tt} - \left(u_{r,rr} + \frac{u_{r,r}}{r} - \frac{u_r}{r^2}\right) = S(u_r, u_{r,r}, u_{r,rr}),$$

$$S(u_r, u_{r,r}, u_{r,rr}) = -\tilde{N}_1 u_{r,rr} u_{r,r} - \tilde{N}_2 \frac{1}{r} u_{r,rr} u_r - \tilde{N}_3 \frac{1}{r^2} u_{r,r} u_r - \tilde{N}_4 \frac{1}{r} (u_{r,r})^2 - \tilde{N}_5 \frac{1}{r^3} (u_r)^2,$$

$$\tilde{N}_1 = 3 + \frac{2(A + 3B + C)}{\lambda + 2\mu}, \quad \tilde{N}_2 = \frac{\lambda + 2B + 2C}{\lambda + 2\mu}, \quad \tilde{N}_3 = \frac{\lambda}{\lambda + 2\mu},$$

$$\tilde{N}_4 = \frac{2\lambda + 3\mu + A + 2B + 2C}{\lambda + 2\mu}, \quad \tilde{N}_5 = \frac{2\lambda + 3\mu + A + 2B + C}{\lambda + 2\mu}. \tag{4}$$

To solve the linear equation (3), we introduce a potential $\Phi(r,t)$ by the formula $u_r = \Phi_{,r}$. Then Eq. (3) becomes simpler:

$$\Phi_{,tt} - (v_L)^2 \left[\Phi_{,rr} + (1/r)\Phi_{,r} \right] = 0. \tag{5}$$

This equation has a solution in the form of a product of harmonic function and the solution of the equation

$$\hat{\Phi}_{,rr} + (1/r)\hat{\Phi}_{,r} + (k_L)^2 \hat{\Phi} = 0. \tag{6}$$

The solution of the Bessel equation (6) is the Hankel function of the first kind and zero order dependent on the radius. Therefore, the solution of Eq. (5) has the form

$$\Phi(r,t) = A_o \; H_0^{(1)}(k_L r) e^{i\omega t}, \tag{7}$$

where A_o is given in the condition $\sigma_{rr}(r_o,t) = p_o e^{i\omega t}$ on the cavity surface $r = r_o$ as an amplitude factor

$$A_o = -\frac{p_o k_L}{k_L(\lambda + 2\mu) H_0^{(1)}(k_L r_o) - \dfrac{2\mu}{r_o} H_1^{(1)}(k_L r_o)},$$

$k_L = (\omega / v_L)$ is the wave number.

Mathematical Background. The classical Bessel equation has the form

$$X'' + (1/x)X' + [1 - (\lambda^2 / x^2)]X = 0. \tag{8}$$

One of the solutions of this equation is expressed in terms of a cylindrical function of a real argument, which is the Hankel function $H_0^{(1)}(x)$ of the first kind and the first order λ.

One of the cylindrical function of an imaginary argument, which is the Macdonald function $K_\lambda(x)$, is one of the solutions of the equation

$$X'' + (1/x)X' - [1 + (\lambda^2 / x^2)]X = 0. \tag{9}$$

If the nonlinear equation (4) is solved by the method of successive approximations, then the first two approximations of the solution is as follows [2, 6, 19]:

$$u_r(r,t) = u_r^{(1)}(r,t) + u_r^{(2)}(r,t), \tag{10}$$

where the first approximation $u_r^{(1)}(r,t)$ is the solution of the linear equation (6):

$$u_r^{(1)}(r,t) = \left[A_o \; H_0^{(1)}(k_L r) e^{i\omega t} \right]_{,r} = -A_o k_L \; H_1^{(1)}(k_L r) e^{i\omega t}. \tag{11}$$

The second approximation can be found in different ways. An analysis of this ways shows [1–4] that four of the five nonlinear terms in (4) that include the factors r^{-1}, r^{-2}, r^{-3} have a weak effect on the final result with distance from the cavity; therefore, the nonlinear terms multiplying these factors can be neglected. Using the approximate representation of the Hankel function and simplification (4) yields the second approximation. Thus, the general solution (7) has the form

$$u_r(r,t) = u_o \; H_1^{(1)}(k_L r) e^{i\omega t} + (u_o)^2 k_L \frac{\tilde{N}_1}{\lambda + 2\mu} H_0^{(1)}(k_L r) H_1^{(1)}(k_L r) e^{2i\omega t}. \tag{12}$$

2. Approximate Solution Found by the Method of Limitation of the Displacement Gradient for a Solitary Cylindrical Nonlinear Elastic Wave with Profile Described by the Macdonald or Friedlander Function.

Consider Eq. (2), ignore only two of the five nonlinear terms, and retain the expression

$$-\widetilde{N}_1 u_{r,rr} u_{r,r} - \widetilde{N}_3 \frac{1}{r^2} u_{r,r} u_r - \widetilde{N}_4 \frac{1}{r} (u_{r,r})^2$$

on the right-hand side of (4). Let represent Eq. (4) in the form

$$u_{r,rr}(1-\widetilde{N}_1 u_{r,r}) + \frac{1}{r} u_{r,r}(1-\widetilde{N}_4 u_{r,r}) - \frac{u_r}{r^2}(1-\widetilde{N}_3 u_{r,r}) - \frac{1}{(c_L)^2} u_{r,tt} = 0.$$

Considering the precedent mentioned above, we approximately assume that $\widetilde{N}_1 \approx \widetilde{N}_3 \approx \widetilde{N}_4$ and obtain the nonlinear wave equation

$$(v_L)^2 (1-\widetilde{N}_1 u_{r,r}) \left(u_{r,rr} + \frac{1}{r} u_{r,r} - \frac{u_r}{r^2} \right) - u_{r,tt} = 0. \quad (13)$$

Let us first consider the linear version of Eq. (13):

$$(v_L)^2 \left(u_{r,rr} + \frac{1}{r} u_{r,r} - \frac{u_r}{r^2} \right) - u_{r,tt} = 0. \quad (14)$$

Recall that the goal of analysis of Eq. (13) is to analyze solitary waves. However, despite the difference between solitary and harmonic waves, we will use the experience of analysis of a harmonic wave and introduce a potential as follows:

$$u_r(r,t) = \Phi_{,r}(r,t). \quad (15)$$

Then Eq. (14) can be written as

$$\Phi_{,tt} - (v_L)^2 \left[\Phi_{,rr} + (1/r)\Phi_{,r} \right] = 0. \quad (16)$$

Let the candidate solution of Eq. (16) have the form of a solitary wave:

$$\Phi_{(L)}(r,t) = \Phi_r^o F_{(L)}(r - v_L t) = u_r^o F_{(L)}(\sigma_L). \quad (17)$$

Substituting solution (17) into Eq. (16) yields equations for the unknown function $F_{(L)}$:

$$\left[F''_{(L)} + \frac{1}{r} F'_{(L)} - \left(1 + \frac{1}{r^2} \right) F_{(L)} \right] = 0. \quad (18)$$

Equation (18) is a partial case of the Bessel equation (9) and has a solution expressed in terms of the Macdonald function $K_1(x)$:

$$\Phi_{(L)}(r,t) = \Phi_{(L)}^o K_1(r - v_L t) = \Phi_{(L)}^o K_1(\sigma_L). \quad (19)$$

We now return to the nonlinear equation (13) for a cylindrical radial wave, which has the same structure as the nonlinear equation for a plane longitudinal wave. It has the form of a linear equation with variable velocity that depends on the solution of the wave equation. This is a feature of a simple wave [4, 6, 9, 19].

To simplify the analysis, we introduce a potential according to formula (15) and rearrange Eq. (13) as

$$\Phi_{,tt} - (v_L)^2 (1 - \widetilde{N}_1 \Phi_{,rr}) \left[\Phi_{,rr} + (1/r)\Phi_{,r} \right] = 0. \quad (20)$$

Let the candidate solution of Eq. (20) have the form of a solitary wave with initial profile (initial condition for the wave equation) that can be described by a known (given) function $\Phi(r, t=0) = \Phi^o F(r)$. Then a wave generated in this way can be represented as

$$\Phi(r,t)=\Phi^o F(r-vt)=\Phi^o F(\sigma) \quad (21)$$

with unknown phase variable σ and unknown wave velocity:

$$v=\sqrt{1-\tilde{N}_1\Phi_{,rr}}\; v_L=\sqrt{1-\tilde{N}_1\Phi^o F_{,rr}}\; v_L \quad (22)$$

and known (given) constant initial amplitude factor Φ^o.

Formula (21) allows transforming the linear version of Eq. (20) to an ordinary differential equation with respect to radius (18). Given condition (21), this equation has solution (19):

$$\Phi(r,t)=\Phi^o K_1(r-vt)=\Phi^o K_1(\sigma). \quad (23)$$

Noteworthy is the following difference between formulas (19) and (23): the velocity is constant and known in the former and variable and unknown in the latter.

Let us apply the method of limitation of the displacement gradient and retain the first two approximations. The procedure of finding an approximate solution of is described in [20, 22–27], where the necessary limitations for the parameters of the problems are indicated as well:

the condition of approximate representation of the variable velocity in the form

$$v=\left(1-(1/2)\tilde{N}_1\Phi^o F_{,rr}\right)v_L; \quad (24)$$

$$|\tilde{N}_1\Phi^o F_{,rr}|<1, \quad (25)$$

$$\left|\delta^* =-(1/2)ac_L\alpha_1 u_{r,r}t\right|<1. \quad (26)$$

Formulas (25), (26) include limitations for three known quantities (one is the length a of the solitary wave, another is its velocity c_L in linear approximation, and the third α_1 is related to material characteristics) and unknown displacement gradient $u_{r,r}(r,t)$. Then wave (17) can be described by the approximate formula

$$u_r(r,t)\approx u_r^o F(\sigma)-(1/2)a^2(u_r^o)^2 c_L\alpha_1 t[F'(\sigma)]^2. \quad (27)$$

This formula has two terms that can be considered as the first two approximations: one is the solution of the classical linear equation and the other is quadratically nonlinear as regards the initial profile.

Let us now consider two examples where the function $F[a(r-vt)]$ describes solitary waves with specific initial profiles. These profiles are described by formulas (1) and (2). These are the $K_\lambda(r)$ [29, 30] and the Friedlander function $F(r)=A^o e^{-br/x_{att}}(1-r/x_{att})$ [9, 10].

Substituting the Macdonald function $F(\sigma)=K_0(\sigma)$ into (27), we get

$$u_r(r,t)\approx u_r^o K_0\left(a(r-c_L t)\right)-(1/2)a^2(u_r^o)^2\alpha_1 ac_L t\left[K_1\left(a(r-c_L t)\right)\right]^2. \quad (28)$$

Formula (28) describes the change of the initial wave profile using the direct dependence of the nonlinear term on time.

With the Friedlander function

$$F(\sigma)=A^o e^{-b\sigma/x_{att}}(1-\sigma/x_{att})$$

solution (27) takes the form

$$u_1(x_1,t)=u_r^o e^{-ba(r-c_L t)/x_{att}}\left[1-a(r-c_L t)/x_{att}\right]$$

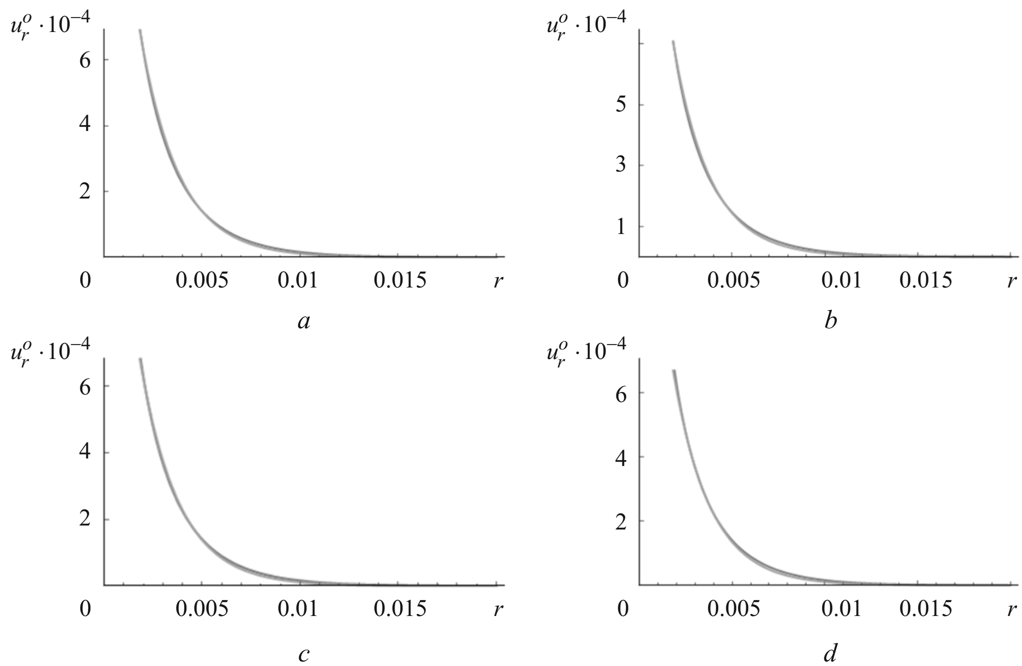

Fig. 1

$$-(1/2)\alpha a^2 c_L t (1/x_{att})^2 (u_r^o)^2 \left\{1 + b\left[1 - a(r - c_L t)/x_{att}\right]\right\}^2 e^{-2ba(r-c_L t)/x_{att}} . \tag{29}$$

Formula (29) describes the change of the initial wave profile using the direct dependence of the nonlinear term on time.

3. Comparison of the Evolution Scenarios for Solitary Cylindrical Nonlinear Elastic Waves with Macdonald and Friedlander Initial Profiles.

Formulas (16) and (17) make it possible to analyze numerically the evolution of cylindrical waves with two different profiles. More exactly, these profiles are very similar graphically, yet very different mathematically. Our goal here is to numerically establish the evolution scenarios of both profiles and find out whether they will be different because of the difference of the mathematical descriptions.

Evolution scenarios were determined for four composted materials described by the Murnaghan model with the following mechanical parameters [1, 2, 6, 12, 16–19, 28]: density ρ; Lame constants (constants of the second order) λ, μ; Murnaghan constants (constants of the third order A, B, C.

Material 1: aluminum matrix with a volume fraction of 0.8 and tungsten reinforcement

$$\rho = 0.594 \cdot 10^{-4}, \quad \lambda = 5.59 \cdot 10^{-10}, \quad \mu = 3.26 \cdot 10^{-10},$$

$$A = -0.658 \cdot 10^{-11}, \quad B = -2.18 \cdot 10^{-11}, \quad C = -4.35 \cdot 10^{-11}, \quad c_L = 4.515 \cdot 10^3 .$$

Material 2: aluminum matrix with a volume fraction of 0.6 and tungsten reinforcement

$$\rho = 0.918 \cdot 10^{-4}, \quad \lambda = 11.6 \cdot 10^{-10}, \quad \mu = 0.721 \cdot 10^{-10},$$

$$A = -1.33 \cdot 10^{-11}, \quad B = -4.45 \cdot 10^{-11}, \quad C = -9.5 \cdot 10^{-11}, \quad c_L = 3.769 \cdot 10^3 .$$

Material 3: tungsten matrix with a volume fraction of 0.2 and copper reinforcement

$$\rho = 0.179 \cdot 10^{-4}, \quad \lambda = 4.26 \cdot 10^{-10}, \quad \mu = 0.363 \cdot 10^{-10},$$

$$A = -73.1 \cdot 10^{-10}, \quad B = -29.1 \cdot 10^{-10}, \quad C = -3.43 \cdot 10^{-10}, \quad c_L = 5.278 \cdot 10^3 .$$

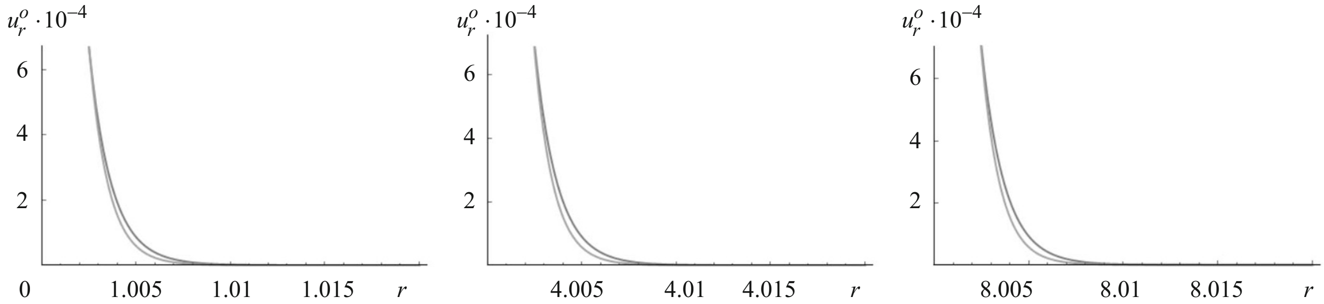

a *b* *c*

Fig. 2

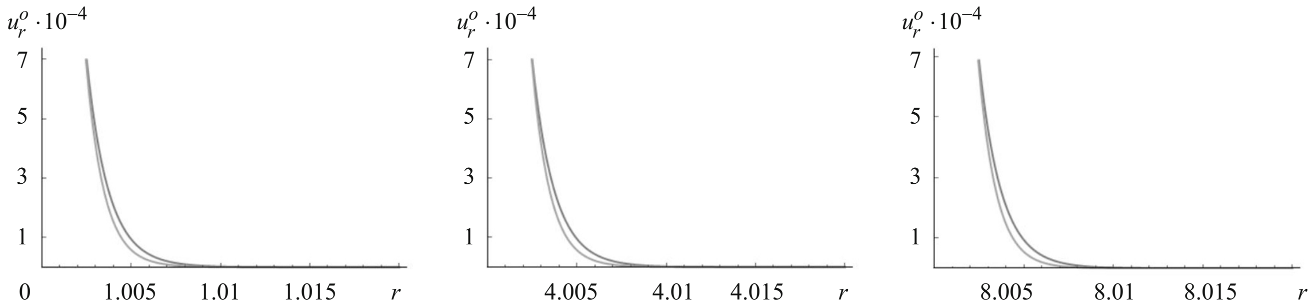

a *b* *c*

Fig. 3

Material 4: molybdenum matrix with a volume fraction of 0.8 and tungsten reinforcement

$$\rho = 0.378 \cdot 10^{-4}, \quad \lambda = 0.022 \cdot 10^{-10}, \quad \mu = 0.042 \cdot 10^{-10},$$

$$A = -19.58 \cdot 10^{-11}, \quad B = -17.04 \cdot 10^{-11}, \quad C = -15.34 \cdot 10^{-11}, \quad c_L = 0.532 \cdot 10^{3}.$$

Since the numerical analysis based on formulas (16) and (17) is multiparameter, the final results depend not only on the chosen material, but also on the time of propagation of the wave, its length, and the maximum amplitude of the initial profile. To make the graph of the Friedlander profile closer to that of the Macdonald profile, we choose parameters $b = 2.5 \cdot 10^{2}$, $x_{att} = 2 \cdot 10^{-2}$ for the former.

First, it is necessary to compare the Friedlander and Macdonald profiles as the solutions of the linear equation (23). To this end, the Macdonald function is considered as the exact solution of Eq. (23). Since the graph of the Friedlander function is similar to that of the Macdonald function, the former can be considered as an approximated solution of Eq. (23). To determine the degree of closeness of the graphs of the Friedlander and Macdonald functions for the four materials, the graphs have been drawn using parameters corresponding to these materials. These graphs are shown in Figs. 1*a*,*b*,*c*,*d* for materials *1*, *2*, *3*, *4*, respectively.

It can be seen from Figs. 1*a*–*d* that there are certain parameter values for which the graphs of the Friedlander and Macdonald functions are very similar. Since the Macdonald function is the exact solution and the graphs of both functions are close, we can conclude that the chosen Friedlander functions are approximate solutions of Eq. (23). This conclusion leads to the other conclusion that representing the solution as a solitary wave (21) is possible for the Friedlander function as an approximation of the Macdonald function. Note that the mathematical descriptions of these functions are very different.

Figures 2–5 show three graphs each (*a*, *b*, *c*) for two profiles corresponding to solutions (16) and (17). Figures 2–5 correspond to materials *1*–*4*.

Note that Fig. 1 represents the starting moment of wave motion and shows the initial wave profiles.

Figures 2*a*–5*a* represent the time it takes the wave to travel a distance equal to 50 wave lengths. Figures 2*c*–5*c* represent the time it takes the wave to travel a distance equal to 400 wave lengths approximately.

The lower graph corresponds to the Macdonald profile, and the upper graph to the Friedlander profile.

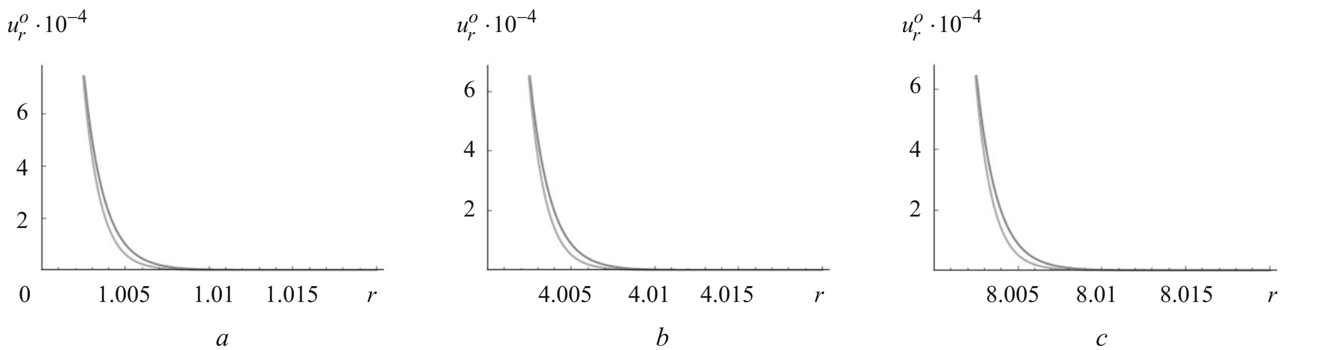

Fig. 4

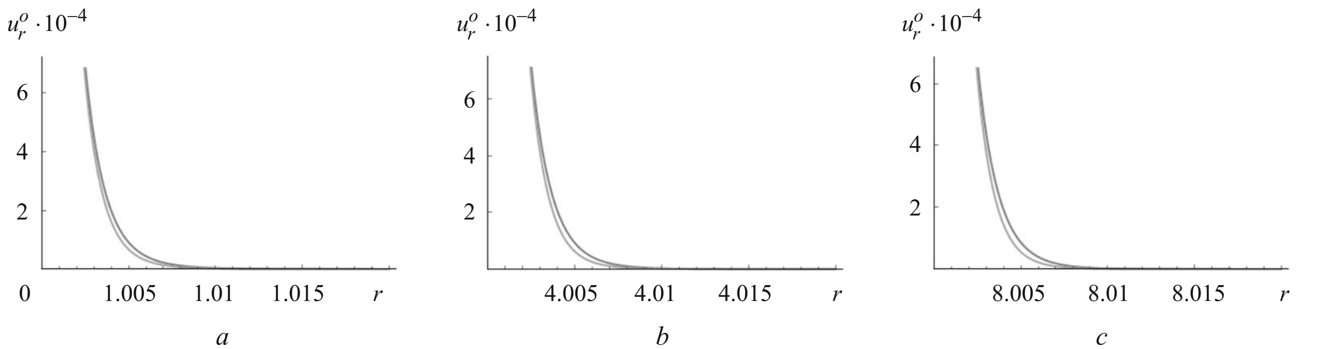

Fig. 5

For each material, the following three main parameters were determined: initial amplitude $A^o = 1 \cdot 10^{-3}$, wave length $a = 0.02$, wave velocity c_L.

The figures below show wave profiles as the dependence of the wave amplitude u_r^o on the radius *r*.

All the graphs demonstrate that the wave evolves from the very beginning of motion because of the nonlinearity of the propagation medium: the wave becomes more convex.

Figures 2*a*–5*a* show not only this nonlinear effect of increasing convexity, but also the distortion of both profiles at the initial stage of propagation, the difference between the graphs being small.

Figures 2*b*,*c*–5*b*,*c* demonstrate the convexity of both profiles continues to increase with time of travel, but the difference between them remain unchanged and small.

Thus, our theoretical analysis and numerical modeling have shown that the evolution scenarios of the profiles are very similar. Hence, both profiles are interchangeable despite the fact that their mathematical descriptions are different.

General Conclusions. We have analyzed theoretically and numerically the propagation of a nonlinear elastic cylindrical radial displacement wave for an arbitrary solitary wave profile and two initial wave profiles in the form of the Macdonald and Friedlander functions. The theoretical basis of the analysis is the Murnaghan nonlinear five-constant model. Unlike the majority of nonlinear waves in materials that have periodic or single humps, these wave profiles do not have hump, decrease monotonically, and are convex downward. Comparing the Macdonald and Friedlander profiles as the solutions of the linear wave equation has shown that if the Macdonald function is considered as the exact solution of this equation, then the Friedlander function can be considered an approximate solution of this equation because its graphical representation is similar to that of the Macdonald function. To determine the degree of closeness for the chosen four materials, the graphs of the Friedlander and Macdonald functions have been drawn.

The graphs lead to the conclusion that representing the solution as a solitary wave is possible for the Friedlander function as an approximation of the Macdonald function. It should be noted once again that the mathematical descriptions of these functions are very different. The wave evolution has been analyzed using the approximate method of limitation of the displacement gradient and retaining the first two approximates. We have derived formulas for an approximate representation of a solitary cylindrical wave and specific representations of waves with Friedlander and Macdonald profiles. Thus, our theoretical analysis and numerical modeling have shown that the evolution scenarios of the profiles are very similar. Hence, both profiles are interchangeable despite the fact that their mathematical descriptions are different.

REFERENCES

1. A. N. Guz, *Elastic Waves in Prestressed Bodies* [in Russian], in two vols., Naukova Dumka, Kyiv (1986).
2. L. K. Zarembo and V. A. Krasil'nikov, *Introduction to Nonlinear Acoustics* [in Russian], Nauka, Moscow (1966).
3. A. I. Lurie, *Nonlinear Theory of Elasticity*, North-Holland, Amsterdam (1990).
4. J. J. Rushchitsky, "On approximate analysis of the evolution of a compression wave propagating in an elastic medium," *Dop. NAN Ukrainy*, No. 8, 46–58 (2019).
5. J. J. Rushchitsky, "Atypical evolution of a solitary wave propagating in a nonlinear elastic medium," *Dop. NAN Ukrainy*, No. 12, 34–58 (2020).
6. J. J. Rushchitsky and S. I. Tsurpal, *Waves in Microstructural Materials* [in Ukrainian], Inst. Mekh. S. P. Timoshenka, Kyiv (1998).
7. M. Alonso and N. Reguera, "Numerical detection and generation of solitary waves for a nonlinear wave equation," *Wave Motion*, **56**, 137–146 (2015).
8. D. Beli, J. R. F. Arruda, and M. Ruzzene, "Wave propagation in elastic metamaterial beams and plates with interconnected resonators," *Int. J. Solids Struct.*, 139–140, 105–120 (2018).
9. C. Cattani and J. Rushchitsky, *Wavelet and Wave Analysis as applied to Materials with Micro and Nano-structure*, World Scientific, Singapore–London (2007).
10. N. Chandra, S. Ganpule, N. N. Kleinschmit, R. Feng, A. D. Holmberg, A. Sundaramurthy, V. Selvan, and A. Alai, "Evolution of blast wave profiles in simulated air blasts: experiment and computational modeling," *Shock Waves*, **22**, 403–415 (2012).
11. F. G. Freidlander, "The diffraction of sound pulses. I. Diffraction by a semi-infinite plate," *Proc. Roy. Soc. London*, *A*, **186**, 322–344 (1946).
12. I. A. Guz and Y. Y. Rushchitskii, "Comparison of mechanical properties and effects in micro- and nano-composites with carbon fillers (carbon microfibers, graphite microwhiskers, and carbon nanotubes)," *Mech. Comp. Mater.*, **40**, No. 3, 179–190 (2004).
13. Y. Ishii, S. Biwa, and T. Adachi, "Second-harmonic generation of two-dimensional elastic wave propagation in an infinite layered structure with nonlinear spring-type interfaces," *Wave Motion*, **97**, No. 9, 102569 (2020).
14. M. Kuriakose, M. Skotak, A. Misistia, S. Kahali, A. Sundaramurthy, and N. Chandra, "Tailoring the blast exposure conditions in the shock tube for generating pure, primary shock waves: The end plate facilitates elimination of secondary loading of the specimen," *PLoS ONE*, **11**, No. 9, e0161597 (2016).
15. L. N. Li, Y. Z. Wang, and Y. S. Wang, "Three-dimensional nonreciprocal transmission in a layered nonlinear elastic wave metamaterial," *Int. J. Non-Linear Mech.*, **125**, No. 10, 193531(2020).
16. F. Murnaghan, *Finite Deformation in an Elastic Solid*, 3rd ed. Gloucester, Peter Smith Publisher Inc., MA, USA (1985).
17. J. J. Rushchitsky, *Theory of Waves in Materials*, Ventus Publishing ApS, Copenhagen (2011).
18. J. J. Rushchitsky, "Certain class of nonlinear hyperelastic waves: classical and novel models, wave equations, wave effects," *Int. J. Appl. Math. Mech.*, **8**, No. 6, 400–443 (2012).
19. J. J. Rushchitsky, *Nonlinear Elastic Waves in Materials*, Springer, Heidelberg (2014).
20. J. J. Rushchitsky, "Plane Nonlinear Elastic Waves: Approximate Approaches to Analysis of Evolution," Chapter in the book W. A. Cooper (ed.), *Understanding Plane Waves*, Nova Science Publishers, London (2019), pp. 201–220.
21. J. J. Rushchitsky, *Foundations of Mechanics of Materials*, Ventus Publishing ApS, Copenhagen (2021).
22. J. J. Rushchitsky, "Scenarios of evolution of some types of simple waves in nonlinear elastic materials," *Archive of Appl. Mech.*, **91**, No. 7, 3151–3170 (2021).
23. J. J. Rushchitsky, C. Cattani, and S. V. Sinchilo, "Physical constants for one type of nonlinearly elastic fibrous micro- and nanocomposites with hard and soft nonlinearities," *Int. Appl. Mech.*, **41**, No. 12, 1368–1377 (2005).
24. J. J. Rushchitsky and V. M. Yurchuk, "One approximate method for analyzing solitary waves in nonlinearly elastic materials," *Int. Appl. Mech.*, **52**, No. 3, 282–290 (2016).

25. J. J. Rushchitsky and V. M. Yurchuk, “Numerical analysis of the evolution of plane longitudinal nonlinear elastic waves with different initial profiles,” *Int. Appl. Mech.*, **53**, No. 1, 104–110 (2017).
26. J. J. Rushchitsky and V. M. Yurchuk, “Effect of the third approximation in the analysis of the evolution of a nonlinear elastic P-wave. Part 1,” *Int. Appl. Mech.*, **56**, No. 5, 581–589 (2020).
27. J. J. Rushchitsky and V. M. Yurchuk, “Effect of the third approximation in the analysis of the evolution of a nonlinear elastic P-wave. Part 2,” *Int. Appl. Mech.*, **56**, No. 6, 666–673 (2020).
28. V. Hauk (ed.), *Structural and Residual Stress Analysis*, Elsevier Science B. V., Amsterdam (1997); e-variant (2006).
29. V. N. Yurchuk and J. J. Rushchitsky, “Numerical analysis of evolution of the plane longitudinal nonlinear elastic waves with different initial profiles,” *Int. App. Mech.*, **53**, No. 1, 104–110 (2017).
30. V. M. Yurchuk, J. J. Rushchitsky, O. M. Hryhorchuk, and Ya. V. Symchuk, “Noncharacteristic evolution of a nonlinear elastic single cylindrical wave,” *Int. App. Mech.*, **57**, No. 6, 619–634 (2021).